Journal of Electrotechnology, Electrical Engineering and Management (2023)
Clausius Scientific Press, Canada
DOI: 10.23977/jeeem.2023.060507
ISSN 2560-6697 Vol. 6 Num. 5

Optimization Design of a Solar Mirror Field Based on an Optimization Model

Wenkai Jia[1,a,*], Yinlong Yang[1,b], Liangzhou Tian[1,c]

[1]*Department of Mechanical Engineering, Shanxi Institute of Technology, Yangquan, Shanxi, China*
[a]*17335836684@189.cn*, [b]*yangyinlong2022@163.com*, [c]*tlz859@outlook.com*
[*]*Corresponding author*

Keywords: Cutoff Efficiency, Cosine Efficiency, Analytic Hierarchy Process, Genetic Algorithm, Simulated Annealing Algorithm

Abstract: Solar thermal power generation is an advanced and environmentally friendly clean energy technology of the 21st century. It harnesses solar energy to produce electricity by concentrating sunlight to create high-temperature environments, converting this heat energy into usable thermal energy, and then transforming it into electrical energy. This makes it suitable for meeting basic electricity needs, especially in the context of renewable energy integration and energy storage. However, solar tower power plants also face several challenges, including high construction and maintenance costs, dependence on geographical location and weather conditions, and energy storage issues. Additionally, they often require extensive land use and cannot generate power continuously during cloudy conditions or at night. This paper delves into discussions and research on how to address these two aspects of the problem, leveraging the power of mathematical modeling for practical problem solving.

1. Introduction

In response to achieving the 'carbon peak' and 'carbon neutrality' goals, the construction of a new electricity system using renewable energy sources is a crucial initiative. Solar thermal power generation is an advanced and environmentally friendly clean energy technology of the 21st century. It harnesses solar energy to produce electricity by concentrating sunlight to create high-temperature environments, converting this heat energy into usable thermal energy, and then transforming it into electrical energy. The key advantage of solar thermal power systems is their ability to generate controlled power output as needed, not solely relying on direct sunlight. This makes them suitable for fulfilling basic electricity demands, especially in the context of renewable energy integration and energy storage. Furthermore, this technology enables efficient thermal storage, allowing continuous power generation during nighttime or low sunlight conditions. Heliostats, which are large parabolic or trough-shaped mirrors, serve as the fundamental components for capturing solar energy. They are designed to focus sunlight onto a receiver at the top of a tower. These mirrors are typically quite large to capture as much sunlight as possible, thereby enhancing energy conversion efficiency.

H. Sheykhlou et al. [1] evaluated the design and performance of a low-cost biaxial solar tracking

system for centralized photovoltaic applications. In the study, [2] carried out the optimal design of a parabolic trough solar collector based on computational fluid dynamics (CFD).The performance of linear Fresnel solar collector and the optimal design of non-uniform mirror are studied [3]. In this study, a high concentration non-imaging optical solar collector is developed and optimized [4]. The optimal design and performance analysis of a solar parabolic trough collector with high-order non-uniform tube spacing are carried out [5]. This evaluated the performance of the centralized solar collector and optimized the design [6]. A high concentration photovoltaic solar system with non-imaging optical elements is designed and its performance is evaluated [7]. In this study, the microstructure parabolic trough collector is optimized to be suitable for high concentration photovoltaic systems [8]. The performance of a low concentration photovoltaic thermal solar collector is simulated and designed [9]. This study analyzed and optimized the performance of parabolic trough collectors in southern Tunisia [10].

In the first step of this article, a hierarchical analysis model is used to visualize the collected data. Data calculations are performed using relevant formulas to obtain the optical efficiency of each heliostat, annual average optical efficiency, and annual average output thermal power. Next, certain parameter values are specified within appropriate ranges, and a genetic algorithm is employed to find the data solution. A suitable model is established to maximize the annual average output thermal power per unit mirror area while meeting the design requirements. Finally, assuming that the dimensions of the heliostats and installation heights can vary, various parameters of the heliostat field are redefined. An intelligent algorithm's simulated annealing model is developed to maximize the annual average output thermal power per unit mirror area, while ensuring that the heliostat field meets the rated power conditions. The results are then evaluated and calculated.

2. Model Establishment and Solution

2.1. Analytic Hierarchy Process Model

For this helioscope problem, we decide to establish an analytic hierarchy process model in order to visualize the obtained data.

2.1.1. Establishment of the Analytic Hierarchy Process Model

First, establish the heliostat field model using MATLAB and obtain the result as shown in Figure 1.

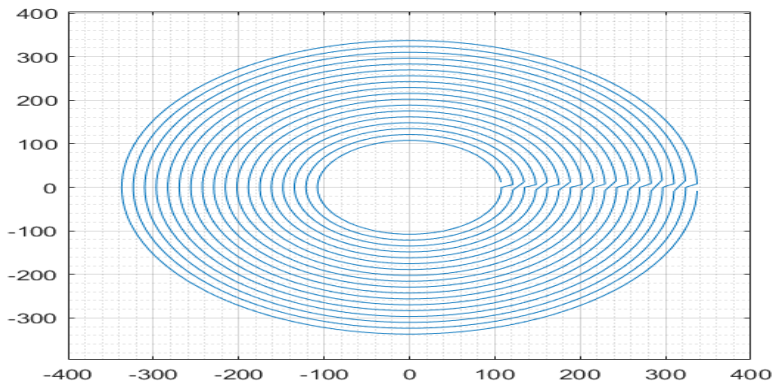

Figure 1: Heliostat Neighbors Diagram

The optical efficiency of the heliostat field is closely related to the solar altitude angle and solar azimuth angle. To calculate the average optical efficiency and average output thermal power, it is

essential to calculate the solar altitude angle and solar azimuth angle, which can be determined using the following equations:

$$\sin\alpha_s = \cos\delta\cos\varphi\cos\omega + \sin\delta\sin\omega \tag{1}$$

$$\sin\gamma_s = \frac{\sin\delta - \sin\alpha_s\sin\varphi}{\cos\alpha_s\cos\varphi} \tag{2}$$

$$\omega = \frac{\pi}{12}(ST - 12) \tag{3}$$

$$\sin\delta = \sin\frac{2\pi D}{365}\sin(\frac{2\pi}{360}23.45) \tag{4}$$

$$E_{field} = \mathrm{DNI}\cdot\sum_{i}^{n}\mathrm{A}_i\eta_i \tag{5}$$

Utilize MATLAB to visualize the solar azimuth angle and solar altitude angle. For all 'annual average' indicators in this problem, calculations are performed at local times on the 21st day of each month at 9:00, 10:30, 12:00, 13:30, and 15:00. Since the month and time are fixed, the corresponding direct normal irradiance per unit time per unit area is determined accordingly. Based on the calculation formula for heliostat optical efficiency:

$$\eta = \eta_{sb}\eta_{\cos}\eta_{at}\eta_{trunc}\eta_{ref} \tag{6}$$

The cosine efficiency ($\eta_{\cos}$), atmospheric transmissivity (η_{at}), and mirror reflectance (η_{ref}) are assumed to be constant under the given latitude conditions. According to the assumed model and the results shown in Figure 5.2, it is observed that shadow shading only occurs during two time periods: 9:00-10:30 and 13:30-15:00, for three months. Assuming a shadow shading loss of 0.01, the shadow shading efficiency (η_{sb}) is also constant at 0.99. Therefore, the optical efficiency of the heliostats (η) is only related to the collector truncation efficiency (η_{trunc}). According to the calculation formula for collector truncation efficiency:

$$\eta_{trunc} = \frac{Energy\ Received\ by\ the\ Receiver}{Energy\ of\ Mirror\ Total\ Reflection - Energy\ Loss\ due\ to\ Shadow\ Shading} \tag{7}$$

Since the shadow shading loss is 0.01, the energy loss due to shadow shading can be considered negligible. The collector truncation efficiency is solely related to the energy received by the collector and the energy reflected by the mirrors. Visualize the shadow shading loss to obtain Figure 2.

Simultaneously, we can obtain the relationships between direct normal irradiance, solar azimuth angle, and solar altitude angle with respect to the change in months, as depicted in Figures 3, 4, and 5, respectively.

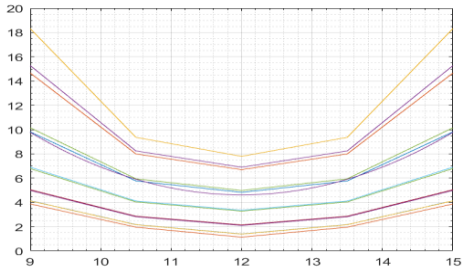

Figure 2: Relationship between Shadow Shading Loss and Local Time Variation

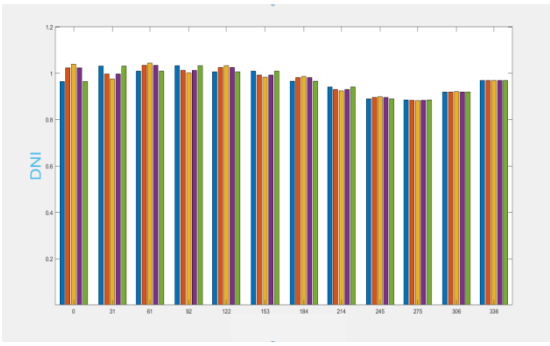

Figure 3: Relationship between Direct Normal Irradiance and Month Variation

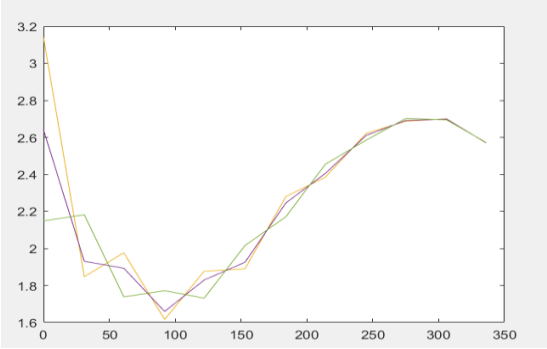

Figure 4: Relationship between Solar Azimuth Angle and Month Variation

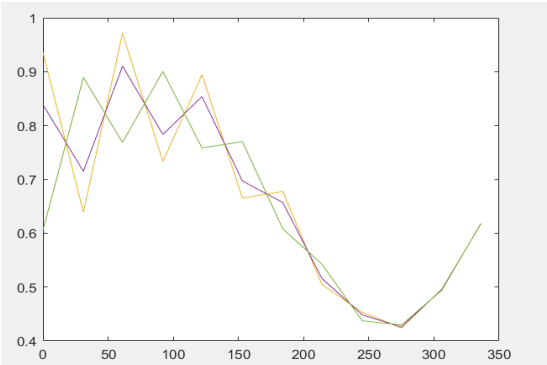

Figure 5: Relationship between Solar Altitude Angle and Month Variation

2.1.2. The Factors Influencing Shadow Shading Loss

From Figure 2, it is visually evident that when the distance between the centers of adjacent heliostat bases is 11m, shadow shading only occurs during 9:00 and 15:30 for 3 months out of the

year. Compared to the overall calculations, this portion of shadow shading loss has a minimal impact on the optical efficiency of heliostats under this condition. However, to ensure more reliable results in subsequent model establishment and calculations, we can assume a shadow shading loss of 0.01.

2.1.3. Solving with Analytic Hierarchy Process Algorithm

For solving the Analytic Hierarchy Process Algorithm, a sensitivity analysis model was established to mathematically transform the real-world problem. Using the established model, calculations were performed, and the results were summarized to obtain Table 1.

Table 1: Annual Average Optical Efficiency and Output Power

Annual Average Optical Efficiency	Annual Average Cosine Efficiency	Annual Average Shadow Shading Efficiency	Annual Average Truncation Efficiency	Annual Average Output Thermal Power(*MW*)	Unit Area Mirror Annual Average Output Thermal Power(kW/m^2)
0.60	0.78	0.99	0.84	36.31	0.58

2.2. Establishment and Solution of Genetic Algorithm Models

2.2.1. Determination of Basic Parameters

According to the design requirements, in order to achieve the rated power for the heliostat field and maximize the unit mirror area's annual average output thermal power, it is necessary to minimize energy losses and reduce shadow shading losses as much as possible. According to the predictive model, it was found that when the distance between the centers of adjacent heliostat bases is 7m, with a mirror width and height of 2m, the corresponding shadow shading loss is nearly zero, and the shadow shading efficiency is approximately 1. The relationship between the parameters and local time is shown in Figure 6-Figure 8.

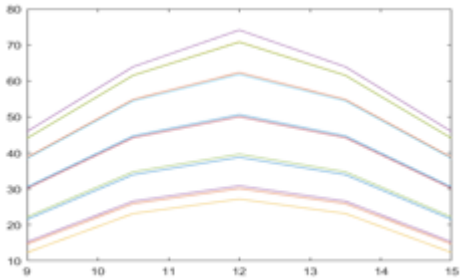

Figure 6: Shadow Shading Variation on Local Time for an Installation Height of 4m

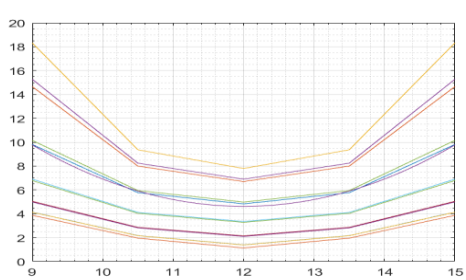

Figure 7: Shadow Shading Variation with Local Time for an Installation Height of 4m

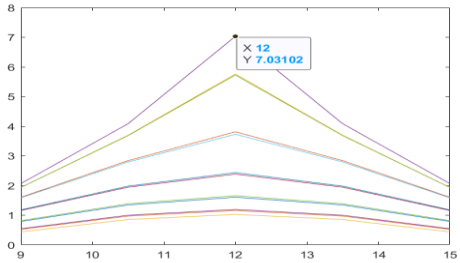

Figure 8: Shadow Shading Variation with Local Time for an Installation Height of 2m

2.2.2. The Establishment of Genetic Algorithm

Based on Figure 6, DNI exhibits a basic symmetric structure with respect to local time. Calculating the solar azimuth and altitude angles can be achieved using the collected data, typically through solar position models or relevant algorithms. Cosine efficiency is assumed to be constant for the given time.

In this study, a parametric model is defined to represent the installation position of heliostat. Genetic algorithms are used to reduce the dimension of the data and search for the best installation location, which may include the coordinates, tilt Angle and orientation of the heliostat.

2.2.3. Evaluation of Results

The obtained results were input into the established hierarchical analysis model for evaluation, and the output thermal power reached 60.2 *MW*, meeting the design requirements, as detailed in Table 2 and Table 3.

Table 2: Annual Average Optical Efficiency and Output Power with Design Parameters

Annual Average Optical Efficiency	Annual Average Cosine Efficiency	Annual Average Shadow Shading Efficiency	Annual Average Truncation Efficiency	Annual Average Output Thermal Power(*MW*)	Unit Area Mirror Annual Average Output Thermal Power(kW/m^2)
0.63	0.69	1.00	1.00	60.20	6.90

Table 3: Heliostat Design Parameters

Coordinates of the Absorption Tower Location	Heliostat Dimensions (Width ×Height)	Heliostat Installation Height(m)	Total Number of Heliostats	Total Mirror Area(m^2)
(0,0)	2.0×2.0	7.00	2181	8724

2.3. Establishment of the Simulated Annealing Model

According to the design requirements, the goal is to achieve the rated power for the solar concentrator field while maximizing the annual average thermal power output per unit mirror area. To achieve this, efforts are made to minimize energy losses and reduce shadowing losses. Based on the predictive annealing model, it was found that the optimal relative distance between the centers of adjacent solar concentrator bases is 9.6m. This corresponds to a mirror width of 4.6m and a mirror height of 4m, resulting in the maximum annual average thermal power output per unit mirror area.

In this study, the obtained data are substituted into the genetic algorithm model established before to search for the best installation position of heliostat. The obtained results were evaluated with the analytic hierarchy model to ensure that they met the design requirements, as shown in Table 4 and Table 5.

Table 4: Annual Average Optical Efficiency and Output Power for Different Heliostat Sizes

Annual Average Optical Efficiency	Annual Average Cosine Efficiency	Annual Average Shadow Shading Efficiency	Annual Average Truncation Efficiency	Annual Average Output Thermal Power(*MW*)	Unit Area Mirror Annual Average Output Thermal Power(kW/m^2)
0.61	0.78	0.99	0.84	123.81	0.44

Table 5: Design Parameters for Different Heliostat Sizes

Coordinates of the Absorption Tower Location	Heliostat Dimensions (Width ×Height)	Heliostat Installation Height(m)	Total Number of Heliostats	Total Mirror Area(m^2)
(0,0)	4.6×4.0	9.6	1274	23441.6

$$\eta_{cos} = \cos\theta = \frac{(b_n + \sin\alpha_s h + x\cos\alpha_s \sin\gamma_s + y\cos\alpha_s \sin\gamma_s)^{1/2}}{(2b_n)^{1/2}} \tag{8}$$

By using the above formula (8), the value of the cosine efficiency of the heliostat can be accurate, the final data can be more accurate, and the model can be more reasonably close to the actual situation.

3. Conclusion

3.1. Result Analysis

(1)Using the established model, the results show that the annual average optical efficiency of the solar field is 0.60, and the annual average thermal output is 36.31 *MW*. The annual average thermal output per unit mirror area is 0.58 kW/m^2.

(2) Based on the formulated data, predictions were made for all data points. It was found that using solar mirrors with a width and height of 2 m each meets the requirement of achieving the rated annual average thermal output of 60 *MW*. The predicted values were then evaluated, resulting in a unit mirror area's annual average thermal output of 6.90 kW/m^2.

(3) Using data and annealing predictions, it was determined that solar mirrors with dimensions of 4.6 x 4 m meet the requirement of achieving the rated annual average thermal output of 60 *MW*. The predicted values were evaluated, resulting in an annual average thermal output of 123.81 *MW* for the solar mirrors.

3.2. Advantages and Disadvantages of Models

3.2.1 .Advantages and Disadvantages of Genetic Algorithms

Genetic algorithms possess a robust global search capability, allowing them to explore large search spaces and facilitate the discovery of global optima solutions close to the global optimum. This makes them perform well in complex problems. They are typically not very sensitive to the choice of initial conditions and parameters, meaning they can perform well across different

problems and settings without extensive parameter tuning. Additionally, genetic algorithms can search for multiple local optima in solution space, making them suitable for multimodal optimization problems where multiple local optima exist.

However, genetic algorithms tend to find better local optima but do not guarantee finding the global optimum. In some cases, the algorithm may get stuck in a local optimum and struggle to escape it. Genetic algorithms often involve multiple parameters such as population size, crossover rate, mutation rate, etc. Selecting appropriate parameter values is crucial for algorithm performance but requires experience or tuning.

3.2.2. Advantages and Disadvantages of the Annealing Model

The simulated annealing algorithm has several adjustable parameters, such as initial temperature, temperature reduction rate, and neighborhood search strategy. These parameters can be adjusted based on the problem's characteristics to optimize the algorithm's performance. The core idea of the algorithm is to mimic the annealing process of materials, gradually reducing the temperature to dynamically adapt to the problem's characteristics during the search process. This enables it to perform well for different types of problems and problem structures. Additionally, the simulated annealing algorithm can search for multiple local optima of a problem, making it suitable for multimodal optimization problems where multiple possible solutions exist.

Similarly, this algorithm has several disadvantages. The convergence speed of the simulated annealing algorithm is typically slower than some other optimization algorithms, especially in high-dimensional problems. It requires a sufficient number of iterations to gradually decrease the temperature and explore the search space. The simulated annealing algorithm is sensitive to parameter settings, and different problems may require different parameter configurations. Therefore, when applying it to a new problem, careful parameter selection is necessary.

References

[1] H. Sheykhlou and S. Jafarmadar and S. Khalilarya. (2021). Design and parametric study of a novel solar-driven trigeneration application utilizing a heliostat field with thermal energy storage. International Journal of Energy Research. 45. https://doi.org/10.1002/er.6736.

[2] S. M. Alirahmi and A. Khoshnevisan and P. Shirazi and P. Ahmadi and D. Kari. (2022). Soft computing based optimization of a novel solar heliostat integrated energy system using artificial neural networks. Sustainable Energy Technologies and Assessments. https://doi.org/10.1016/j.seta.2021.101850.

[3] N. Pai and H. Yau and Tzu-Hsiang Hung and C. Hung. (2013). Application of CMAC Neural Network to Solar Energy. Heliostat Field Fault Diagnosis. https://doi.org/10.1155/2013/938162.

[4] Song Yang and Jun Wang and P. Lund. (2020). Optical Design of a Novel Two-Stage Dish Applied to Thermochemical Water/CO2 Splitting with the Concept of Rotary. Secondary Mirror Energies. https://doi.org/10.3390/en13143553.

[5] Lifang Li and A. Kecskemáthy and A. Arif and S. Dubowsky. (2011). Optimized Bands: A New Design Concept for Concentrating. Solar Parabolic Mirrors. 133. https://doi.org/10.1115/1.4004351.

[6] James E. Harvey and A. Krywonos and Patrick L. Thompson and Timo T. Saha. (2001). Grazing-incidence hyperboloid-hyperboloid designs for wide-field x-ray imaging applications. Applied Optics. 40 (1). https://doi.org/10.1364/AO.40.000136.

[7] Shuai Shao and Xuemei Zhu and Yijie Fan. (2019). A Study on Cosine Efficiency in a Tower Reflector Solar Power System ACM .Cloud and Autonomic Computing Conference. https://doi.org/10.1109/CAC48633.2019.8996808.

[8] Xiaoyan Zhao and Suying Yan and N. Zhang and Ningyu Zhao and Hongwei Gao. (2022). Solar Flux Measuring and Optical Efficiency Forecasting of the Linear Fresnel Reflector Concentrator after Dust Accumulation. Journal of Thermal Science. 31. https://doi.org/10.1007/s11630-022-1596-7.

[9] S. Shaaban. (2021). Enhancement of the solar trough collector efficiency by optimizing the reflecting mirror profile. International Journal of Energy Research. 176.

[10] Poļikarpova and Roberts Kaķis and Ieva Pakere and D. Blumberga. (2021). Optimizing Large-Scale Solar Field Efficiency: Latvia Case Study. Energies. https://doi.org/10.3390/en14144171.